Original Paper

phys. stat. sol. (b) **244**, No. 4, 1219–1226 (2007) / **DOI** 10.1002/pssb.200674510

Dual composite right/left-handed (D-CRLH) leaky-wave antenna with low beam squinting and tunable group velocity

Christophe Caloz[*, 1], **Samer Abielmona**[1], **Hoang Van Nguyen**[1], and **Andre Rennings**[2]

[1] École Polytechnique de Montréal, 2500, ch. de Polytechnique Montréal, Québec, H3T 1J4, Canada
[2] IMST GmbH, Carl-Friedrich-Gauss-Str. 2, 47475 Kamp-Lintfort, Germany

Received 14 October 2006, revised 31 October 2006, accepted 27 November 2006
Published online 22 March 2007

PACS 41.20.Jb, 81.05.Zx, 84.30.–r, 84.40.Az

The propagation and radiation properties of dual composite right/left-handed (D-CRLH) transmission line metamaterials are presented, and validated experimentally with a 1D microstrip prototype. In its fast-wave regime, this structure operates as a leaky-wave antenna capable of backfire-to-endfire radiation scanning with beam squinting smaller than that of conventional CRLH (C-CRLH) antennas. It is shown that this D-CRLH beam squinting can be further reduced by increasing the group velocity but that this can occur, close (and possibly beyond) to luminal velocities, only at the expense of losses produced by parasitic effects, a fundamental limitation which is demonstrated via the Bloch impedance concept.

1 Introduction

Over the past decade, electromagnetic metamaterials have spurred considerable excitement in the physics and engineering communities [1–3]. Two main families of metamaterials have been explored: the resonant-type structures, typically constituted of split ring resonators and thin wires [1, 4], and the transmission line metamaterials, constituted of non-resonant lumped elements [2, 5, 6]. The latter, in addition to lower loss, exhibit a much broader bandwidth, and their phase response may therefore be manipulated to design novel devices with unprecedented properties [2], a new area of electromagnetics sometimes referred to as *dispersion engineering*.

The paper describes the low beam squinting and tunable group velocity properties of the novel dual CRLH (D-CRLH) transmission line metamaterials, analyzed in [7] and demonstrated experimentally in [8], and their fast-wave regime operation as leaky-wave antennas.

2 Ideal D-CRLH characteristics

The equivalent circuit model for an ideal D-CRLH transmission line metamaterial is shown in Fig. 1(a). The fundamental waveguiding properties of the D-CRLH have been derived in [7] and [8]. We briefly recall them here for the sake of completeness. The per-unit-length impedance Z' and admittance Y' of the D-CRLH are

$$Z' = \frac{1}{1/(j\omega L'_{\mathrm{R}}) + j\omega C'_{\mathrm{L}}} = j\frac{\omega L'_{\mathrm{R}}}{1-(\omega/\omega_{\mathrm{se}})^2}, \qquad Y' = \frac{1}{1/(j\omega C'_{\mathrm{R}}) + j\omega L'_{\mathrm{L}}} = j\frac{\omega C'_{\mathrm{R}}}{1-(\omega/\omega_{\mathrm{sh}})^2}, \tag{1}$$

[*] Corresponding author: e-mail: christophe.caloz@polymtl.ca, Phone: +1 514 340 4711, ext. 3326, Fax: +1 514 340 5892

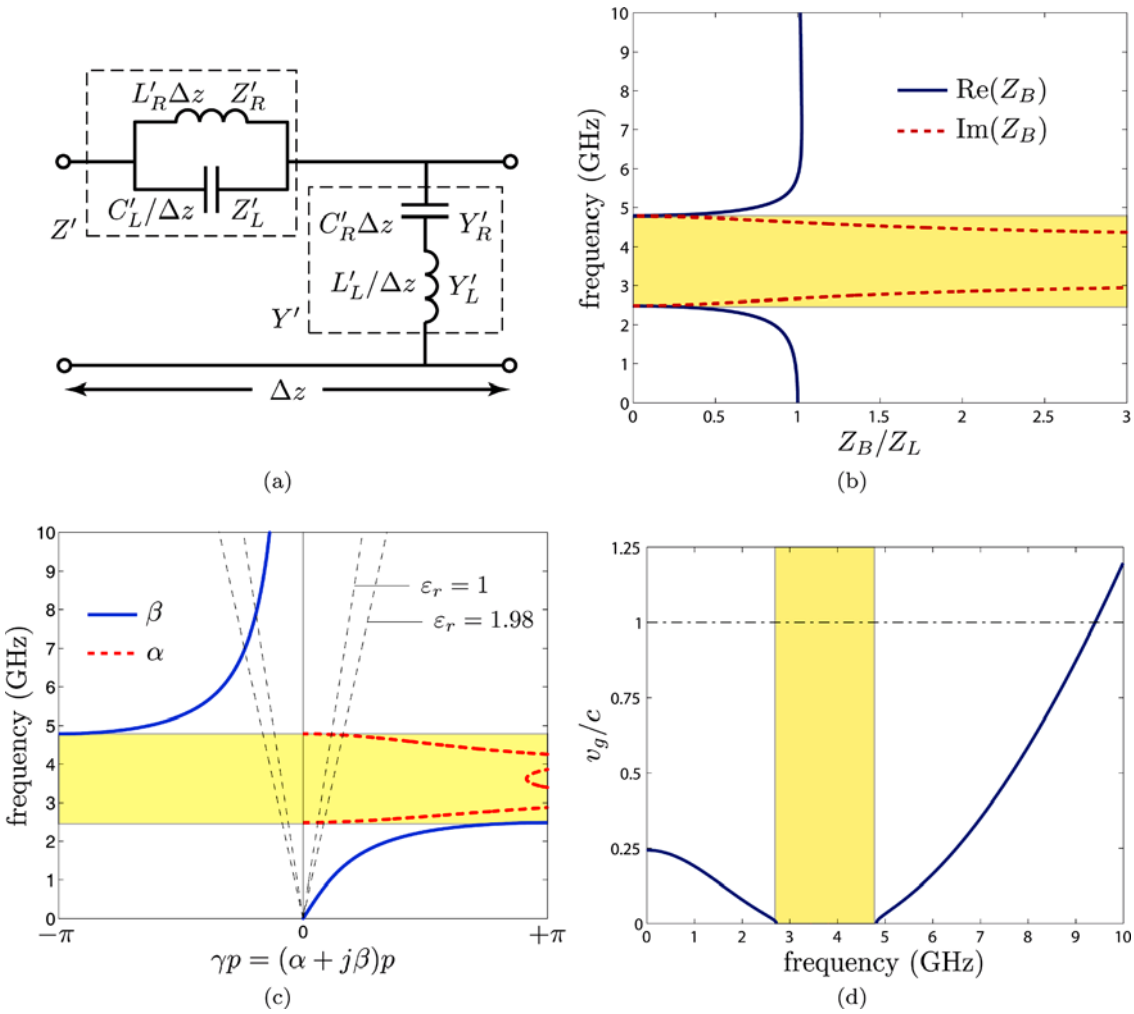

Fig. 1 (online colour at: www.pss-b.com) Ideal D-CRLH transmission line metamaterial characteristics. (a) 1D circuit model (readily extendible to 2D and 3D). (b) Normalized Bloch impedance, Z_B/Z_L ($Z_L = \sqrt{L_L/C_L}$) [Eq. (2a)]. (c) Dispersion and attenuation diagrams, $\beta(\omega)$ and $\alpha(\omega)$ [Eq. (2a)]. (d) Normalized group velocity $v_g(\omega)/c$. The parameter values for figures (b), (c) and (d) are $L_R = 2.5$ nH, $C_R = 1$ pF, $L_L = 1.75$ nH, $C_L = 0.85$ pF. The air line ($\varepsilon_r = 1$) and equivalent dielectric line ($\varepsilon_r = 1.98$) [effective permittivity of the microstrip structure to be presented in Section 3] are also shown for the period of $p = 144$ mil (3.66 mm).

where $\omega_{se} = 1/\sqrt{L_R C_L}$ and $\omega_{sh} = 1/\sqrt{L_L C_R}$ represent the resonance frequencies of the series and shunt tanks, respectively. Such a homogeneous (i.e. infinitesimally uniform) transmission medium does not exist naturally; it is therefore constructed artificially under the form of a ladder network of electrically small ($\Delta z/\lambda_g \ll 1$) D-CRLH unit cells with the inductance and capacitance elements ($L'_R\,\Delta z, C'_R\,\Delta z$, $L'_L/\Delta z, C'_L/\Delta z$). By applying Bloch–Floquet theorem to the transmission matrix of the D-CRLH unit cell expressed in terms of the impedance $Z'\,\Delta z$ and admittance $Y'\,\Delta z$ [2], the complex propagation constant γ and Bloch impedance Z_B [2] are obtained as

$$\gamma(\omega) = \frac{1}{p}\cosh^{-1}\left(1 - \frac{\xi}{2}\right), \quad \text{with} \quad \xi = \frac{1}{(\omega_R/\omega)^2 + (\omega/\omega_L)^2 - \kappa\omega_R^2}, \tag{2a}$$

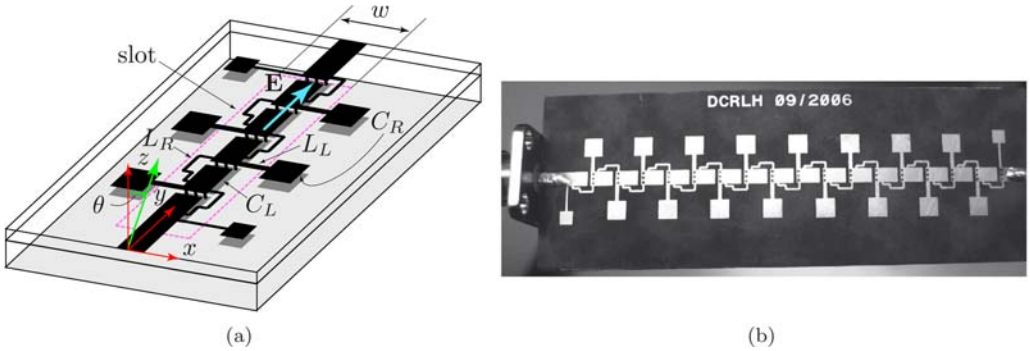

Fig. 2 (online colour at: www.pss-b.com) D-CRLH [Fig. 1(a)] transmission line structure in microstrip technology with printed LC elements. (a) Perspective view showing the three metallization layers, top: microstrip ports, series/shunt inductors (L_R/L_L) and series/shunt capacitor (C_L/C_R) metal-insulator-metal (MIM) top patches, intermediate: patches completing the MIM capacitors with the top layer patches, bottom: ground plane with possible slot, of width w (to be used in Section 6). (b) Prototype constituted of $N=17$ unit cells. Both substates are Duroid 5870 with permittivity of 2.33. The thicknesses of the lower and upper substrates are 20 and 5 mil, respectively. The structure includes $N=17$ cells of size $p=144$ mil (3.6 mm) for an overall length of $\ell = N_p = 2448$ mil (62.2 mm).

$$Z_B(\omega) = \frac{j\omega L_R}{[1-(\omega/\omega_{se})^2]\sqrt{\xi(\xi/4-1)}}. \tag{2b}$$

In addition, the permeability, permittivity and refractive index of the resulting metamaterial structure, which are valid only in the frequency range of effective homogeneity ($\Delta z/\lambda_g \ll 1$), are directly found from the immittances as $\mu(\omega) = Z'/(j\omega)$, $\varepsilon(\omega) = Y'/(j\omega)$ and $n(\omega) = j\sqrt{Z'Y'}/(c\omega)$. Finally, the D-CRLH is in essence a stop-band filter; its cutoff frequencies corresponds to the points where the input impedance of the line becomes imaginary [2] and are given by

$$\omega_{c,R/L} = \omega_0 \sqrt{\frac{[\kappa + 1/(2\omega_R)^2]\,\omega_0^2 \pm \sqrt{[\kappa + 1/(2\omega_R)^2]^2\,\omega_0^4 - 4}}{2}}. \tag{3}$$

Figure 1(b)–(d) show the Bloch impedance, the dispersion/attenuation diagrams and the group velocity for the ideal D-CRLH case. The Bloch impedance becomes constant, and therefore allowing broadband matching, toward low and toward high frequencies, at both sides of the stop band. The most striking difference with the C-CRLH [2] is immediately visible in the dispersion diagram: the positions of the left-handed and right-handed bands are inverted, the former being higher than the latter. Finally, the group velocity, which is bounded in the C-CRLH case, increases superluminally toward infinity (ideal D-CRLH only) in the left-handed band.

3 Practical D-CRLH implementation and characteristics

Figure 2(a) depicts a 1D microstrip implementation of the D-CRLH, while Fig. 2(b) shows a corresponding prototype. As well-known from basic microwave engineering, such a structure is subject to electromagnetic parasitic effects, the influence of which increases with increased frequency.

Figure 3(a) shows the experimental circuit model corresponding to the D-CRLH structure of Fig. 2 including parasitics. This model represents a high frequency extension of the ideal model of Fig. 1(a). The parasitics include two contributions: the *quasi-static parasitics* (essentially a series inductance and two shunt capacitances) of the capacitors (C_R, C_L) and the *dynamic distributed effects* (electrical length non negligible) of the inductors (C_R, C_L). The dispersion diagram of Fig. 3(b) reveals that the presence of

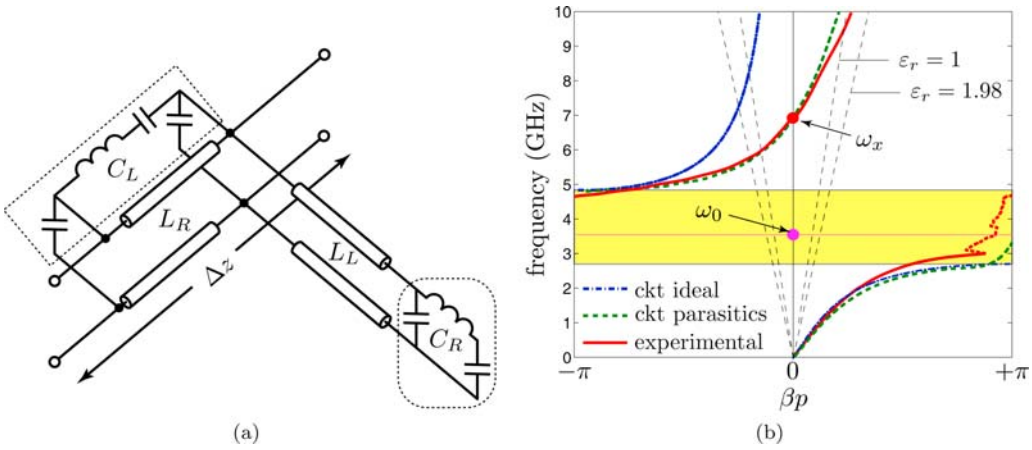

Fig. 3 (online colour at: www.pss-b.com) Practical D-CRLH transmission line metamaterial [Fig. 2] characteristics. (a) Approximate 1D circuit model, including the quasi-static capacitance and distributed inductance parasitics. (b) Dispersion diagram, $\beta(\omega)$, compared with the ideal circuit-model (ckt) curves of Fig. 1(c), where the LC parameters correspond to the extracted values for the prototype of Fig. 2(b), and with the curves for the circuit-model including parasitics (computed by approximate formulas) shown in Fig. 3(a). The air line ($\varepsilon_r = 1$) and equivalent dielectric ($\varepsilon_r = 1.98$) line are also shown for the period of $p = 144$ mil. The triangular area delimited by the air line is the fast-wave region or radiation cone, where the phase velocity is larger than the velocity of light, $v_p > c$.

the (unavoidable) parasitics prevents the LH branch from exhibiting infinite group velocity (slope $\partial\omega/\partial\beta$) at high frequencies and forces the dispersion curve to penetrate into the right-handed region. This behavior is very similar to the response of the C-CRLH [2], except that, for a given set of the four CRLH parameters (L_R, C_R, L_L, C_L), the D-CRLH transition frequency between the left-handed and right-handed bands is located at a significantly higher frequency, $\omega_x \gg \omega_0 = 1/\sqrt[4]{L_R C_R L_L C}$. This fact is of significant practical interest because it will enable the design of leaky-wave antennas with reduced beam squinting, as it will be shown in the next sections.

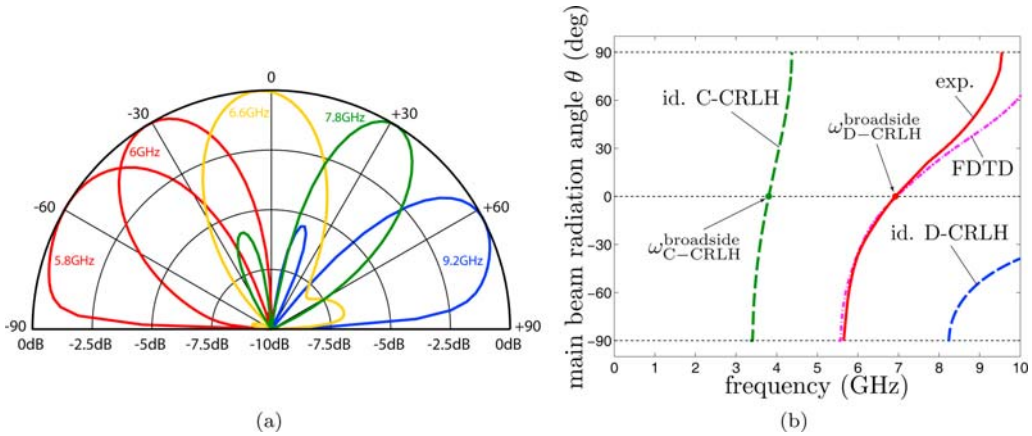

Fig. 4 (online colour at: www.pss-b.com) Leaky-wave antenna performances of the 17-cell D-CRLH structure of Fig. 2(b). (a) Radiation patterns at a few frequency points of the dispersion diagram [Fig. 3(b)]. (b) Experimental (exp.) and ideal (id.) angle-frequency scanning law obtained from the dispersion diagram with the well-known leaky-wave relation $\theta(\omega) = \sin^{-1}[c\beta(\omega)/\omega]$. The law for the C-CRLH with same LC parameters except for C_L, changed from 0.85 pF to 0.7 pF to ensure balancing and subsequent closure of the gap, is also shown for comparison.

4 Leaky-wave antenna operation

As with the C-CRLH, the dispersion curve of the D-CRLH crosses through the fast-wave (or radiation) region, as shown in Fig. 3(b). Consequently, the D-CRLH may also be used as a leaky-wave antenna, with corresponding typically high directivity when the structure is long enough to exhibit a large effective aperture.

Figure 4 shows the radiation response of the D-CRLH. As expected from its dispersion diagram [Fig. 3(b)], the structure is capable of both left-handed backward radiation ($\theta < 0$) and right-handed forward radiation ($\theta > 0$), and it supports in addition a $\beta = 0$ with $v_g \neq 0$ true broadside radiation ($\theta = 0$), so far available for leaky-wave antennas only in C-CRLH structures [2, 9]. Moreover, as previously reported C-CRLH leaky-have antennas [9], this antenna provides backfire-to-endfire radiation capability. But even more interesting is the beam-squinting behavior of this D-CRLH at the broadside radiation angle.

5 Beam squinting

Consider an antenna array with inter-element phase shift $\Delta\phi$ or a metamaterial leaky-wave antenna with inter-cell phase shift $\Delta\phi = \beta p$, where p is the distance between the elements of the array or the period of the metamaterial structure, respectively. The main beam radiation angle θ is related to the free-space wavenumber k_0, p and $\Delta\phi$ by $pk_0 \sin\theta = \Delta\phi = p\beta$ or $\theta(\omega) = \sin^{-1}[c\beta(\omega)/\omega]$, which was used to plot the curves of Fig. 4(b). From this expression, we can easily compute the beam squinting of the antenna, $\zeta(\omega) = \partial\theta/\partial\omega$, which represents the variation in the radiation direction as a function of frequency,

$$\zeta(\omega) = \frac{\partial\theta}{\partial\omega} = \frac{1}{\sqrt{1-(c\beta/\omega)^2}}\left(\frac{\partial\beta}{\partial\omega} - \frac{\beta}{\omega}\right)\frac{c}{\omega} = \frac{1}{\sqrt{1-(c/v_p)^2}}\left[\frac{1}{v_g} - \frac{1}{v_p}\right]\frac{c}{\omega}. \tag{4}$$

At the broadside radiation ($\theta = 0$) frequency, we have $\beta = 0$, i.e. $v_p = \infty$, and therefore this expression reduces to $\zeta(\omega) \approx c/(v_g\omega)$, showing that beam squinting is inversely proportional to the product of the group velocity and frequency. Figure 5 shows the group velocity and beam squinting for the D-CRLH of

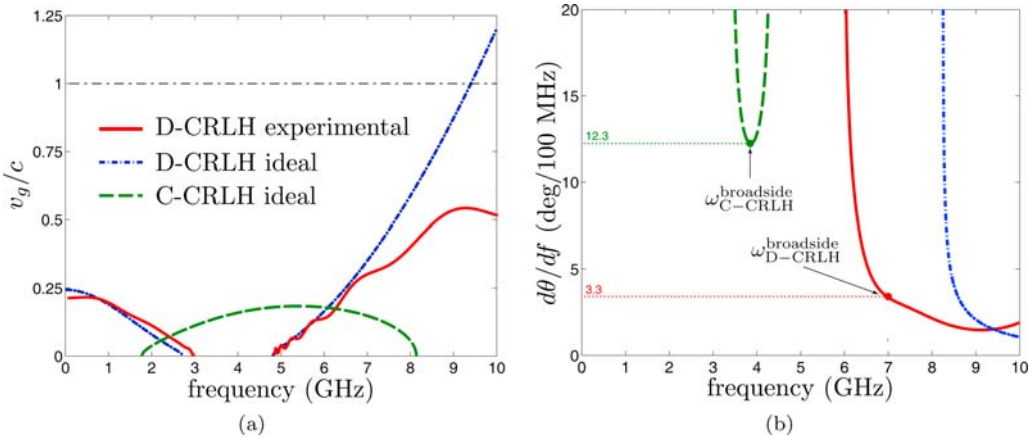

Fig. 5 (online colour at: www.pss-b.com) Group velocity and beam squinting for the D-CRLH transmission line metamaterial prototype of Fig. 2 including comparison with the cases of the ideal D-CRLH and the conventional CRLH (C-CRLH) prototypes with the same parameters as in Fig. 4(b). (a) Group velocity. (b) Beam squinting, computed by Eq. (4).

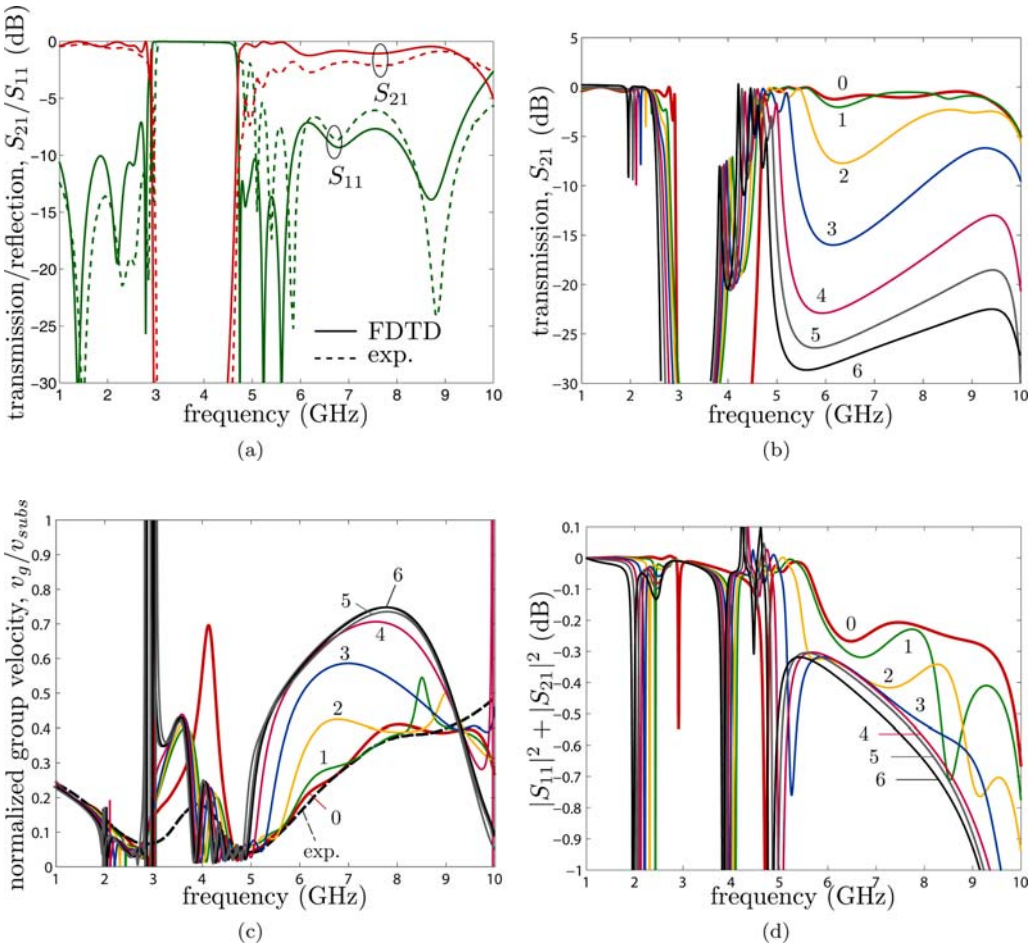

Fig. 6 (online colour at: www.pss-b.com) Group velocity enhancement with the D-CRLH (5-cell) structure of Fig. 2. (a) Experimental validation of the FDTD analysis tool used for the next graphs (case without slots). (b) Insertion loss versus frequency for different slot widths w from 0 (not slot) to 6 mm, as indicated by the labels. (c) Corresponding group velocities. (d) Corresponding levels of $|S_{11}|^2+|S_{21}|^2$ indicating the weak amount of radiation $\xi = 1-(|S_{11}|^2+|S_{21}|^2)$ (no ohmic and dielectric losses). Therefore loss is purely due to mismatch.

Fig. 2, compared to the same quantities for the the ideal D-CRLH and the ideal C-CRLH prototypes with similar LC parameters. Figure 5(a) confirms that, whereas the ideal D-CRLH becomes superluminal at high frequencies, in contrast to the ideal C-CRLH, the practical D-CRLH structure has a bounded group velocity, as a consequence of the parasitic effects described above. Figure 5(b) shows that the broadside squinting of the D-CRLH antenna (here 3.3 deg/100 MHz, occurring 6.9 GHz) is much lower than that broadside squinting of the C-CRLH antenna with similar LC parameters (here 12.3 deg/100 MHz, occurring at 3.8 GHz). This is a consequence of the facts that: (i) the D-CRLH broadside occurs at a higher frequency than the C-CRLH broadside, so that its squinting is more attenuated by the factor $1/\omega$ pointed out above, (ii) the group velocity in the C-CRLH is reduced by the close presence of the right-handed low-pass stop band just above [Fig. 5(a)], whereas no such stop-band exists, at least theoretically, in the D-CRLH case. The lower beam squinting *at the frequency where* $\beta = 0$ is of great practical importance in uniform feeding networks and antenna systems.

6 Group velocity enhancement

Whether beam squinting (in particular at broadside) can be further reduced and, if so, whether there is a fundamental limit to this reduction seem natural questions to ask at this point. Obviously, an ideal D-CRLH structure would exhibit a zero squinting toward high frequencies [Fig. 5(b)] due to its infinite group velocity with finite phase velocity. However, it has been shown in the previous section that such an ideal structure cannot be realized practically due to the presence of parasitic effects; moreover, without these parasitics, this structure would not have the capability of broadside radiation. Is it then possible – and to what extent – to further reduce beam squinting in the practical D-CRLH presented in the previous sections? As seen in Eq. (4), at a given β, beam squinting is minimized by minimizing $\partial\beta/\partial\omega$ or maximizing the group velocity.[1]

Since the group velocity is limited by the parasitic elements [Fig. 3(a)], it should be increased if these elements can be reduced. In the implementation of Fig. 2, the parasitic capacitances to the ground can be reduced by etching out a slot in the ground plane below the axis of the line, as shown in Fig. 2(a). Figure 6, which presents results for different slot widths, demonstrates that the reduction of these parasitic effects indeed induces a dramatic increase in the group velocity [Fig. 6(c)]. However, Fig. 6(b) shows that the larger is the enhancement of v_g, the larger is also the insertion loss. While this occurrence seems in agreement with the established fact that very large (and possibly superluminal) group velocities can be attained only in the presence of large losses [10, 11], consistently with Kramers–Kronig relations, it is interesting to gain further insight in this fundamental limitation in the present case of the D-CRLH structure discussed here.

Figure 7(a) shows a simplified version of the D-CRLH circuit model including parasitics of Fig. 3(a) to address this problem in a more tractable manner. The immittances for this structure are $Z = j\omega L_R(1-\omega^2 L_p C_L)/[1-(\omega/\omega_{sep})^2]$, $\omega_{sep} = 1/\sqrt{[(L_p + L_R)\,C_L]}$ and $Y = j\omega C_p + j\omega C_R/[1-(\omega/\omega_{sh})^2]$, and are recognized as slightly modified versions of the immittances for the ideal case [Eq. (1)]. The Bloch impedance is subsequently modified, as shown in Fig. 7(b) for the case of the widest slot. Comparing this graph with the corresponding S_{21} in Fig. 6(b) reveals that, and how, the parasitic elements strongly

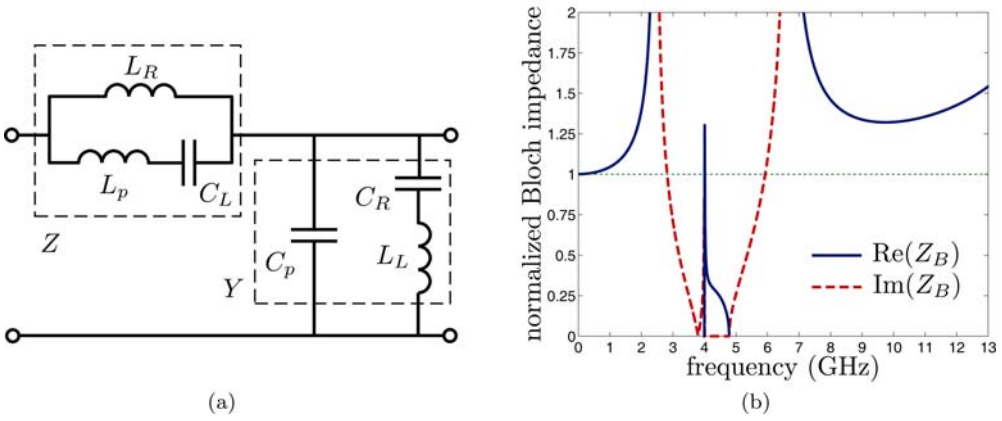

Fig. 7 (online colour at: www.pss-b.com) Explanation of the increasing loss with increasing group velocity from the Bloch impedance. (a) Simplified circuit model including only the dominant parasitic elements, i.e. the parasitic inductance of C_L, L_p, and the parasitic capacitance to the ground for all of the elements, C_p. (b) Corresponding Bloch impedance for the case of a 6 mm slot (Fig. 6), for which $L_p = 1.3$ nH and $C_p = 0.48$ pF, in agreement with Fig. 6(b).

[1] A large group velocity in general, also in the guided-wave region of the dispersion diagram, has the practical interest of providing a large operation bandwidth due to the related small phase variation versus frequency $d\beta/d\omega$.

affect the Bloch impedance, which results in mismatch losses of amounts proportional to the deviation from the nominal (real) impedance of the ports.

7 Conclusions

The propagation and radiation properties of the dual composite right/left-handed (D-CRLH) transmission line metamaterials have been presented and validated experimentally with a 1D microstrip prototype. The structure has been demonstrated as a backfire-to-endfire scanning leaky-wave antenna with a beam squinting much lower than the conventional CRLH antennas, due to larger and tunable group velocity, limited essentially by parasitic effects affecting the Bloch impedance. This D-CRLH may be used with unprecedented performances in various applications such as for instance high-resolution synthetic aperture radar (SAR) systems.

References

[1] D. R. Smith and J. B. Pendry, Reversing light with negative refraction, Phys. Today (June 2004), p. 37.
[2] C. Caloz and T. Itoh, Electromagnetic Metamaterials: Transmission Line Theory and Microwave Applications (Wiley and IEEE Press, 2005).
[3] N. Engheta and R. W. Ziolkowski (eds.), Electromagnetic Metamaterials: Physics and Engineering Explorations (Wiley and IEEE Press, 2006).
[4] D. R. Smith, W. J. Padilla, D. C. Vier, S. C. Nemat-Nasser, and S. Schultz, Phys. Rev. Lett. **84**(18), 4184–4187 (2000).
[5] A. K. Iyer and G. V. Eleftheriades, Negative refractive index metamaterials supporting 2-D waves, in: Proc. IEEE-MTT Internat. Symp., Vol. 2 (Seattle, WA, June 2002), pp. 412–415.
[6] C. Caloz and T. Itoh, Application of the transmission line theory of left-handed (LH) materials to the realization of a microstrip LH transmission line, in: Proc. IEEE-AP-S USNC/URSI National Radio Science Meeting, l. 2 (San Antonio, TX, June 2002), pp. 412–415.
[7] C. Caloz, IEEE Microw. Wireless Compon. Lett. **16**(11), 585–587 (2006).
[8] C. Caloz and H. V. Nguyen, Novel broadband conventional and dual composite right/left-handed (C/D-CRLH) metamaterials: properties, implementation and double-band coupler application, Appl. Phys. A, submitted (2006).
[9] L. Liu, C. Caloz, and T. Itoh, Electron. Lett. **38**(23), 1414–1416 (2002).
[10] L. Brillouin, Wave Propagation and Group Velocity (Academic Press, 1960).
[11] J. D. Jackson, Classical Electrodynamics, 3rd ed. (Wiley, New York, 1998).

